Tetrahedron 71 (2015) 4116–4123

Contents lists available at ScienceDirect

Tetrahedron

journal homepage: www.elsevier.com/locate/tet

A novel switchable [2]rotaxane driven by light energy with Rhodamine B as a stopper

Jiaxin Shi [a,c], Xiaowei Cao [a], Xinlong Wang [c], Xuemei Nie [c], Baojing Zhou [c], Xiaofeng Bao [a,*], Jing Zhu [b,*]

[a] Department of Biochemical Engineering, Nanjing University of Science & Technology, Chemical Engineering Building B308, 200 Xiaolingwei, Nanjing, 210094, PR China
[b] Department of Pharmacy, Nanjing University of Chinese Medicine, 138 Xianlin Dadao, Nanjing, 210023, PR China
[c] School of Chemical Engineering, Nanjing University of Science & Technology, Nanjing, 210094, PR China

ARTICLE INFO

Article history:
Received 31 March 2015
Received in revised form 23 April 2015
Accepted 27 April 2015
Available online 1 May 2015

Keywords:
Rotaxane
Rhodamine B
Synthesis
Fluorescence
Molecular switch

ABSTRACT

Over the past few decades, bistable [2]rotaxanes have been extensively studied because of their applications in molecular switches. In this paper, a rotaxane molecule containing a dibenzo-24-crown-8 ring and Rhodamine B units was synthesized and characterized by ^{1}H NMR and HRMS. The Rhodamine B component allows the fluorophore fluorescence to be manipulated in alternate modes by varying the pH of the solution under irradiation. Because of the easy regulation and high sensitivity of the changes in fluorophore fluorescence, Rhodamine B [2]rotaxane can be used as a molecular switch, with different pH values as the input and changes in the fluorescence intensity as the output signals.

1. Introduction

Rotaxane, a supermolecular compound, is described as a molecular system in which a macrocycle threads a linear axle with two bulky stoppers.[1–4] The macrocycle controls the movement of the ring along the dumbbell-shaped component and reversible molecular motion through changes in the relative positions of the wheels between the two bulky stoppers.[5,6] Because of their unique structural architectures, rotaxanes have shown great promise in a variety of applications, such as molecular sensors, molecular logic gates,[7,8] molecular switches,[9,10] molecular electronic devices[11,12] and drug delivery devices.[13–15] These architectures consist of beautiful interlocking structures and unique mobile features that result from the high degree of freedom among the relatively independent rod and linear components. The shuttling motion of the macrocycle in rotaxane allows for the development of sophisticated supermolecular devices and materials.[16–18]

Recently, supermolecules have been extensively studied for application in the fields of functional molecules and molecular switches, and rotaxanes are unique in that they fluoresce.[19–22] Dyes that contain a fluorescent structure, such as cyclodextrins, 4-morpholin-naphthalimide, and pyrene, have recently been used as a rotaxane cap to study the properties of these supermolecules with electro-optical instruments and, in some cases, even with the naked eye.[23–25] These fluorescent rotaxanes are good models for binary systems because of their variable and reversible fluorescence intensity (output signals), which is controlled by changing the proper external stimuli (input signals).[26–29] For example, using the change in fluorescence as the input ensures that no waste product forms while powering a rotaxane because there are no chemical reactions or changes in the covalent structure.[30–32] Light-driven changes can be easily carried out in small spaces and remotely detected with low cost. These changes are also preferable to other output signals because they are easily transformed into fluorescent output signals, which respond very quickly. However, to the best of our knowledge, there have been few reports on rotaxanes, especially those containing a Rhodamine B moiety.[33]

The design and synthesis of this interlocked molecule presents a significant challenge. Various preparation methods for rotaxanes are being actively pursued based on template-directed strategies using supermolecular interactions, including hydrogen bonding,[34,35] hydrophobic effects,[36–38] electrostatic interactions,[39,40] coordination and ionic templates.[38,39] In practice, however, the use of catalysts or molecular sieves sometimes limits their

* Corresponding authors. E-mail addresses: baoxiaofeng@mail.njust.edu.cn (X. Bao), zhujing1227@hotmail.com (J. Zhu).

http://dx.doi.org/10.1016/j.tet.2015.04.105
0040-4020/

application, and finding a mild and efficient reaction suitable for the synthesis of rotaxanes remains challenging. We previously reported the synthesis of [2]rotaxane and [3]rotaxane by the DCC coupling method.[33,41–44] In this paper, we designed a novel [2]rotaxane (Fig. 1) containing a fluorescence moiety, Rhodamine B, as the bulky stopper. This novel fluorescent [2]rotaxane was efficiently synthesized through the strong hydrogen interactions between the *sec*-ammonium salt axle and the crown ether wheel and the esterification of alcohol with chloride without the help of a catalyst. It was composed of dibenzo-24-crown-8(DB24C8) rings interlocked through a dumbbell-shaped component and 2,2-diphenylacetyl chloride as the other stopper unit. We predominantly focused on the states of the DB24C8 ring in response to external stimuli after the synthesis of [2]rotaxane.

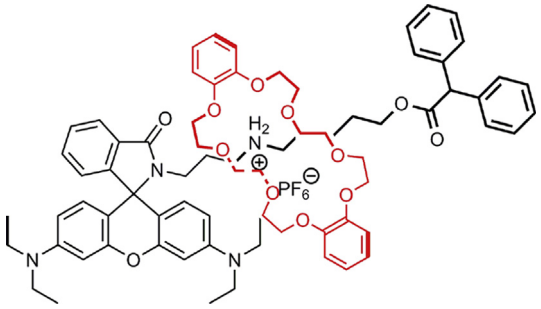

Fig. 1. The chemical structure of Rhodamine B [2]rotaxane.

2. Experimental

2.1. Materials and general methods

All reagents and organic solvents were of ACS grade or higher and used without further purification. Unless otherwise noted, all chemicals were purchased from J&K Scientific (Shanghai, China). Reactions were performed under argon atmosphere with standard Schlenk techniques. Thin-layer chromatography was performed on a HAIYANG silica gel F_{254} plate, and the compounds were visualized under UV light (λ=254 nm). Column chromatography was carried out using HAIYANG silica gel (type: 200–300 mesh ZCX-2). ^{1}H NMR (500 MHz) and ^{13}C NMR (126 MHz) spectra were recorded on an Avance 500 spectrometer (Bruker; Billerica, MA, USA). The chemical shifts are reported in δ units (parts per million) downfield relative to the chemical shift of tetramethylsilane. The abbreviations br, s, d, t and m denote broad, singlet, doublet, triplet and multiplet, respectively. Mass spectra were obtained on a Finnigan TSQ Quantum LC/MS spectrometer. High-resolution mass spectra (HRMS) were acquired with electron impact ionization on a double-focusing high-resolution instrument (Autospec; Micromass Inc.). UV–vis and fluorescence spectra were obtained on a UV-3600 UV–vis-NIR spectrophotometer (Shimadzu, Japan) and an Edinburgh FLS920 fluorescence spectrophotometer (Livingston, UK), respectively, at room temperature.

2.2. Synthesis of 3-(benzyloxy)-3-oxopropan-1-aminium chloride (2)

Hydrogen chloride was prepared by adding concentrated sulfuric acid and sodium chloride to a solution of β-alanine (2.9 g, 32.5 mmol) in 20 mL of phenylmethanol, and the reaction mixture was stirred at room temperature for 15 min. The reaction mixture was stirred at 120 °C for 12 min and then cooled to room temperature. After removal of the solvent under vacuum, the crude product was purified by flash chromatography on silica gel and eluted with CH_2Cl_2/MeOH (v/v, 95:5) to yield compound **2** as a white solid (6.45 g, 92%). ^{1}H NMR (500 MHz, $CDCl_3$, 298K): δ=7.72 (s, 1H), 7.29–7.25 (m, 5H), 5.09 (s, 2H), 3.35 (t, J=5.5 Hz, 2H), 2.92 (t, J=6.5 Hz, 2H) ppm.

2.3. Synthesis of Benzyl3-(3′,6′-bis(diethylamino)-3-oxospiro [isoindoline-1,9′−xanth en]-2-yl)propanoate (3)

A solution of compound **2** (2.00 g, 10 mmol) and triethylamine (1.5 mL, 10.8 mmol) dissolved in 20 mL of CH_2Cl_2 was added to a solution of Rhodamine B (4.00 g, 8.3 mmol) and HOBt (1.2 g, 8.9 mmol) in 30 mL of CH_2Cl_2. After the reaction mixture was stirred at room temperature for 12 h, the solution was filtered through a pad of Celite and then dried under vacuum. The crude mixture was purified by column chromatography using CH_2Cl_2/MeOH (v/v, 98:2) as the eluent to give compound **3** (4.51 g, 90%) as a bright-red solid. ^{1}H NMR (500 MHz, acetone-d_6/D_2O, 298K): δ=7.94–7.92 (m, 1H), 7.58–7.56 (m, 2H), 7.36–7.29 (m, 5H), 7.03–7.01 (m, 1H), 6.43–6.39 (m, 6H), 4.98 (s, 2H), 3.45–3.37 (m, 10H), 2.30 (t, J=7.75 Hz, 2H), 1.15 (t, J=7.0 Hz, 12H) ppm. ^{13}C NMR (126 MHz, acetone- d_6/D_2O, 298 K): δ=171.6, 168.2, 153.9, 153.4, 148.9, 136.0, 132.5, 130.9, 128.9, 128.5, 128.2, 128.0, 123.8, 122.9, 108.3, 105.4, 98.2, 66.2, 65.0, 44.5, 35.9, 32.9, 29.8, 12.7 ppm. HRMS (m/z): $[M+H]^+$ found at 604.3180; calculated for $C_{38}H_{42}N_3O_4^+$, 604.3170.

2.4. Synthesis of 3-(3′,6′-bis(diethylamino)-3-oxospiro[isoindoline-1,9′-xanthen]-2- yl)propanal (4)

Compound **3** (3.75 g, 5.84 mmol) was dissolved in 50 mL of CH_2Cl_2, and the air was purged with nitrogen for 10–20 min in a 100-mL dried round-bottom flask. The solution was cooled to −80 °C, treated with a solution of 1.2 M diisobutylaluminum hydride (DIBAl) in toluene (7.5 mL, 8.76 mmol), and stirred at −80 °C for 2 h under nitrogen. Next, 15 mL of methanol was slowly added to the reaction mixture sequentially, and then, the mixture was stirred at room temperature for another 30 min. The crude mixture was then taken to dryness under vacuum, and the residue was extracted with CH_2Cl_2 (3×40 mL). The combined organic layer was dried with $MgSO_4$ after being concentrated under reduced pressure. Flash chromatography (silica gel; hexane/EtOAc, v/v, 70:30) of the residue yielded compound **4** as a white solid (1.421 g, 49%). ^{1}H NMR (500 MHz, $CDCl_3$, 298 K): δ=9.54 (s, 1H), 7.88–7.90 (m, 1H), 7.42–7.44 (m, 2H), 7.06–7.08 (m, 1H), 6.38–6.44 (m, 4H), 6.27–6.29 (m, 2H), 3.47 (t, J=14.5 Hz, 2H), 3.32–3.36 (m, 8H), 2.35–2.38 (m, 2H), 1.17 (t, J=14.0 Hz, 12H); ^{13}C NMR (126 MHz, $CDCl_3$, 298 K): δ=201.2, 168.2, 153.7, 153.4, 148.9, 132.6, 131.0, 128.8, 128.1, 123.9, 122.8, 108.3, 105.2, 97.9, 65.0, 44.5, 42.65, 34.0, 12.7. HRMS (m/z): $[M+H]^+$ found at 498.2761; calculated for $C_{31}H_{36}N_3O_3^+$, 498.2751.

2.5. Synthesis of 3′,6′-bis(diethylamino)-2-(3-((5-hydroxypentyl)amino)propyl)spiro [isoindoline-1,9′-xanthen]-3-one (5)

Compound **4** (700 mg, 1.41 mmol) was dissolved in 10 mL of CH_2Cl_2, and then, 5-amino-1-pentanol (440 μL, 4.83 mmol) was added to the solution, followed by stirring of the resulting mixture for 3.5 h. $NaBH(OAc)_3$ (598 mg, 2.82 mmol) was added. After the mixture was stirred overnight at room temperature, 5 mL of H_2O was added to the solution, and it was stirred for an additional 20 min. The crude mixture was then taken to dryness under vacuum, and the residue was extracted with CH_2Cl_2 (3×40 mL). The combined organic layer was dried with $MgSO_4$. After being concentrated under reduced pressure, the crude was purified on a silica column with CH_2Cl_2/MeOH (v/v, 90:10) to yield compound **5**

(323 mg, 39%) as a white solid. ^{1}H NMR (500 MHz, $CDCl_3$, 298K): δ=7.95–7.83 (m, 1H), 7.56–7.30 (m, 2H), 7.28 (s, 1H), 7.17–6.95 (m, 4H), 6.39 (t, J=5.4 Hz, 2H), 3.94–1.72 (m, 2H), 3.53–2.17 (m, 8H), 3.53–1.72 (m, 2H), 2.62 (t, J=6.8 Hz, 2H), 2.55 (dt, J=12.7, 6.6 Hz, 2H), 2.48 (t, J=6.4 Hz, 1H), 1.90 (s, 4H), 1.68–1.52 (m, 2H), 1.52–1.18 (m, 2H), 1.18–1.01 (m, 12H). ^{13}C NMR (126 MHz, $CDCl_3$, 298K) δ=168.86, 153.48, 148.99, 132.43, 131.10, 128.75, 128.26, 123.95, 122.90, 108.19, 105.41, 97.84, 77.85, 76.65, 76.35, 65.70, 65.08, 62.11, 48.62, 45.94, 44.45, 38.15, 36.84, 37.26, 36.90, 32.18, 28.30, 28.13, 27.20, 23.03, 12.66 ppm. HRMS (m/z): $[M+H]^+$ found at 585.3811; calculated for $C_{36}H_{49}N_4O_3^+$, 585.3805.

2.6. Synthesis of *N*-(3-(3′, 6′-bis(diethylamino)-3-oxospiro [isoindoline-1,9′-xanthen] -2-yl)propyl)-5-hydroxypentan-1-aminium (6)

Two milliliters of 2 mol/L HCl (aq) was added to the solution of compound **5** (300 mg, 0.513 mmol) in 10 mL of EtOH, and the mixture was stirred at room temperature for 30 min. The solvent was removed under vacuum to yield a red solid. The residue was dissolved in 10 mL of CH_2Cl_2. A saturated NH_4PF_6 aqueous solution was prepared in 1 mL of water and was added to the mixture. The biphasic solution was stirred vigorously for 8 h until the solid had dissolved into the organic layer. The reaction mixture was then dried under vacuum, washed with DCM three times and purified on a silica column with CH_2Cl_2/MeOH (v/v, 80:20) to yield compound **6** (285 mg, 76%) as a red solid. ^{1}H NMR (500 MHz, $CDCl_3$, 298K): δ=7.92 (d, J=6.9 Hz, 1H), 7.72–7.44 (m, 2H), 7.21 (d, J=7.0 Hz, 1H), 6.41 (d, J=2.4 Hz, 2H), 6.30 (dt, J=8.9, 5.6 Hz, 4H), 3.87–3.62 (m, 2H), 3.52–3.29 (m, 8H), 3.25 (dd, J=25.8, 19.8 Hz, 2H), 3.05 (t, J=7.2 Hz, 2H), 2.85–2.61 (m, 2H), 1.99–1.80 (m, 2H), 1.75–1.49 (m, 4H), 1.38 (d, J=35.5 Hz, 2H), 1.19 (t, J=7.0 Hz, 12H). ^{13}C NMR (126 MHz, $CDCl_3$, 298K): δ=168.86, 153.48, 148.99, 132.43, 131.10, 128.75, 128.26, 123.95, 122.90, 108.19, 105.41, 97.84, 77.85, 76.65, 76.35, 65.70, 65.08, 62.11, 48.62, 45.94, 44.45, 38.15, 36.84, 37.26, 36.90, 32.18, 28.30, 28.13, 27.20, 23.03, 12.66 ppm. HRMS (m/z): $[M]^+$ found at 585.3813; calculated for $C_{36}H_{49}N_4O_3^+$, 585.3805. HRMS (m/z): $[M]^-$ found at 144.9646; calculated for PF_6^-, 144.9642.

2.7. Synthesis of *N*-(3-(3′,6′-bis(diethylamino)-3-oxospiro [isoindoline-1,9′-xanthen]-2 -yl)propyl)-5-(2,2-diphenylacetoxy)pentan-1-aminium (7)

Compound **6** (24 mg, 0.0328 mmol) was dissolved in 2 mL of CH_2Cl_2 and stirred in an ice-cooled bath. Diphenylacetyl chloride (11 mg, 0.0492 mmol) was then added, and the mixture was stirred at 0 °C for another 30 min. The reacting mixture was allowed to reach to room temperature. After the mixture was stirred for 8 h, the solvent was removed under vacuum; water (2 mL) was added, and the mixture was extracted by CH_2Cl_2 (3×50 mL) and water (30 mL). The organic layer was dried over anhydrous sodium sulfate and then concentrated. The crude product was purified via column chromatography with CH_2Cl_2/MeOH (v/v, 80:20) to give compound **7** (20 mg, 68%) as a purple solid. ^{1}H NMR (500 MHz, $CDCl_3$, 298K): δ=9.44 (s, 2H), 7.86 (d, J=7.3 Hz, 1H), 7.59–7.42 (m, 2H), 7.38–7.28 (d, 8H), 7.25–7.20 (m, 1H), 7.09–7.13 (d, 1H), 6.38 (d, J=2.5 Hz, 2H), 6.35 (dd, J=33.2, 5.7 Hz, 2H), 886.30–6.20 (m, 2H), 5.04 (s, 1H), 4.18 (t, J=6.4 Hz, 2H), 3.41–3.30 (m, 8H), 3.30–3.23 (m, 2H), 2.81–2.76 (m, 2H), 2.70–2.63 (m, 2H), 1.91–1.82 (m, 3H), 1.74–1.65 (m, 3H), 1.52–1.43 (m, 3H), 1.42–1.35 (m, 3H), 1.28–1.21 (m, 7H), 1.20–1.09 (m, 13H), 0.91–0.8 (m, 4H). ^{13}C NMR (126 MHz, $CDCl_3$, 298K): δ=172.50, 169.89, 153.47, 149.18, 138.69, 135.70, 133.34, 130.20, 129.96, 128.58, 127.22, 125.81, 124.87, 124.80, 124.15, 122.94, 108.26, 104.08, 97.87, 77.26, 77.01, 76.75, 66.28, 64.66, 57.11, 48.03, 44.40, 35.47, 29.68, 27.92, 25.87, 24.87, 22.91, 14.10, 12.51 ppm. HRMS (m/z): $[M]^+$ found at 779.4551; calculated for $C_{50}H_{59}N_4O_4^+$, 779.4536. HRMS (m/z): $[M]^-$ found at 144.9647; calculated for PF_6^-, 144.9642.

2.8. Synthesis of Rhodamine B [2]rotaxane

Compound **6** (100 mg, 0.1368 mmol) and DB24C8 (123 mg, 0.2736 mmol) were dissolved in 5 mL of $CHCl_3$ and stirred in an ice-salt bath for 2 h. Diphenylacetyl chloride (79 mg, 0.342 mmol) was then added, and the mixture was stirred at −10 °C for an additional 2 h. The reacting mixture was allowed to reach room temperature and then stirred for 8 h. Three milliliters of H_2O was then added to the reaction mixture, and it was stirred for an additional 1 h. The crude mixture was then extracted with $CHCl_3$. The organic layer was dried with $MgSO_4$ and concentrated under vacuum. Chromatography of the residue on a silica gel column eluted with CH_2Cl_2/MeOH (v/v, 95:5) gave Rhodamine B [2]rotaxane as a red solid (77 mg, 40% yield). HRMS (m/z): $[M]^+$ found at 1227.6650; calculated for $C_{74}H_{91}N_4O_{12}^+$, 1227.6634.

2.9. Computational studies

Computational studies were carried out to investigate the nature conformation of Rhodamine B [2]rotaxane using the Gaussian 09 software package. The geometries of Rhodamine B [2]rotaxane were optimized using ab initio HF and density functional theory (DFT) calculations. The geometries were first optimized at the HF/3-21G level. The resulting structures were further optimized by DFT calculations using B3LYP with the 6-31G (d, p) basis sets.

3. Results and discussion

3.1. Synthesis of Rhodamine B [2]rotaxane

As shown in Fig. 1, synthetic rhodamine B [2]rotaxane contains a dibenzo-24-crown-8 (DB24C8) ring that is interlocked onto a dumbbell-shaped thread component around the *sec* -ammonium binding site bearing a terminal fluorescent rhodamine B moiety as a stopper. 2,2-diphenylacetyl chloride was used as the other bulky terminal stopper. We divided the synthetic steps into three main routes to obtain Rhodamine B [2]rotaxane, which will now be illustrated in detail.

As illustrated in Scheme 1, aldehyde **4** was first synthesized as a standard substrate according to our previous report.[30] Briefly, compound **2** was prepared at 92% yield by treating compound **1** with 3-aminopropanoic acid and HCl gas at 120 °C for 12 h, which was followed by coupling with Rhodamine B in the presence of DCC, HOBt, and TEA in CH_2Cl_2 at room temperature for 12 h to obtain ester **3** in a 90% yield. Then, ester **3** was reduced by the slow addition of diisobutylaluminum hydride in DCM at −80 °C under nitrogen for 2 h to provide aldehyde **4** in a 49% isolated yield.

The ammonium salt, compound **6**, was prepared from compound **4**, as shown in Scheme 2. Specifically, the aldehyde **4** and 5-amino-1-pentanol were added to a flask, and the obtained light-red Schiff base was then reduced with $NaBH(OAc)_3$ in MeOH in a 39% isolated yield. Treatment of compound **5** with HCl gas in EtOH for 30 min afforded the 6-H-Cl salt. Anion exchange of 6-H-Cl in DCM with a saturated aqueous solution of NH_4PF_6 afforded the *sec* -ammonium salt, compound **6**, in a 76% isolated yield as a pale red solid.

The synthesis, molecular structure, and schematic representation of compound **7**, Rhodamine B [2]rotaxane, are shown in Scheme 3. This synthesis was based on the esterification reaction of an alcohol with chloride without any catalyst. First, DB24C8 was

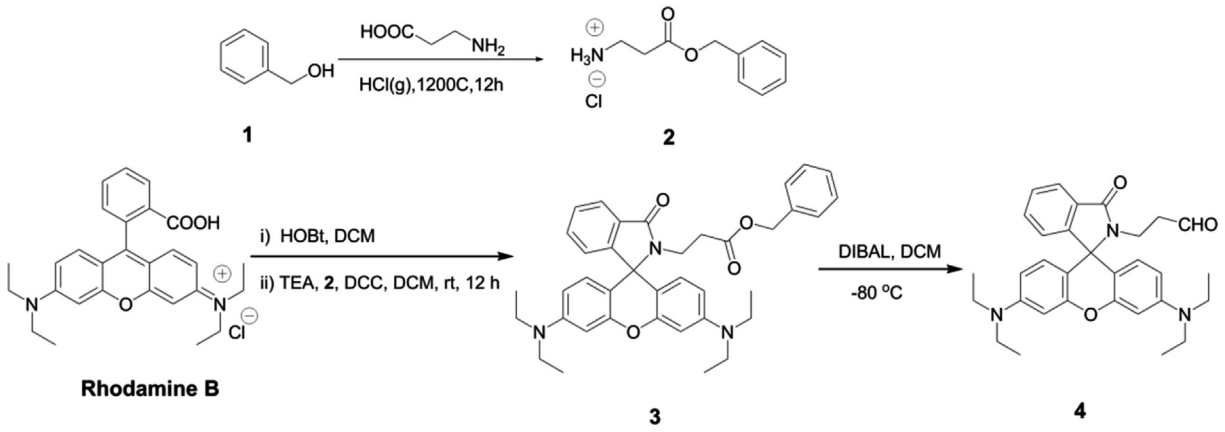

Scheme 1. The synthetic route for compound **4**.

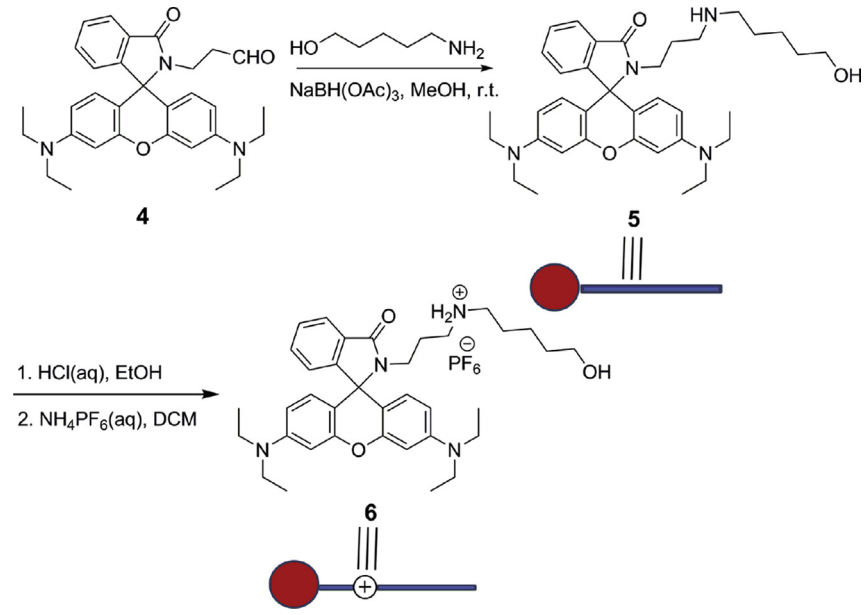

Scheme 2. The synthetic route for componud **6**.

exposed to the compound **6** axle in DCM at −10 °C for 2 h of induced threading, which was followed by the addition of 2,2-diphenylethanamine for another 2 h. The reacting mixture was allowed to reach to room temperature and was then stirred for another 8 h. This mixture was then purified by preparatory silica gel chromatography, and Rhodamine B [2]rotaxane was isolated in a 40% yield as a pale red solid. The product was characterized by ^{1}H NMR and HRMS (Fig. S1). Compound **7** was also synthesized and isolated in a 68% yield by the same method without the addition of DB24C8, and its structure was characterized by ^{1}H NMR and HRMS (Fig. S1), illustrating that this capping method uses mild reaction conditions and simple steps.

To verify the synthesis of Rhodamine B [2]rotaxane, the ^{1}H NMR spectra of compound DB24C8, compound **6**, compound **7** and Rhodamine B [2]rotaxane were compared, and all were in agreement with their structures. The ^{1}H NMR spectrum of compound **6** is shown in Fig. 2a, along with the spectrum observed after the addition of the other stopper (Fig. 2b). Upfield shifts in protons 10, 12 and 16 ($\Delta\delta$=0.109, 0.209 and 0.194 ppm, respectively) were observed, as well as a significant downfield shift in proton 17 ($\Delta\delta$=−0.470 ppm) due to the introduction of the 2,2-diphenylethanamine unit. The single peak of proton 25 also demonstrates the product of compound **7**, indicating that this quick blocking reaction method can be used to block rotaxane. When DB24C8 interlocked on the thread of **7** to form [2]rotaxane, the proton signals of 11 and 14 displayed slight chemical shifts from the multiplet peaks centered at 1.899 and 1.481 ppm to singlet peaks centered at 1.792 and 1.382 ppm, respectively ($\Delta\delta$=0.107 and 0.099 ppm, respectively). These changes were due to the strong hydrogen bond between DB24C8 and the secondary ammonium salt and offer additional proof of this synthetic method's ability to synthesize [2]rotaxane. Moreover, all of the proton peaks belonging to the macrocyclic DB24C8 (21, 22, 23, 24) appeared in Fig. 2d at 4.151, 3.912, 3.835 and 6.884 ppm, respectively, and moved downfield significantly ($\Delta\delta$=0.173, 0.199, 0.226, and 0.070 ppm, respectively) because the macrocyclic ring was interlocked on the dumbbell of **7** to form [2]rotaxane. The axle contained Rhodamine B and 2,2-diphenylethanamine units as two bulky terminal stoppers to prevent unthreading, which further demonstrated that we had successfully synthesized [2]rotaxane.

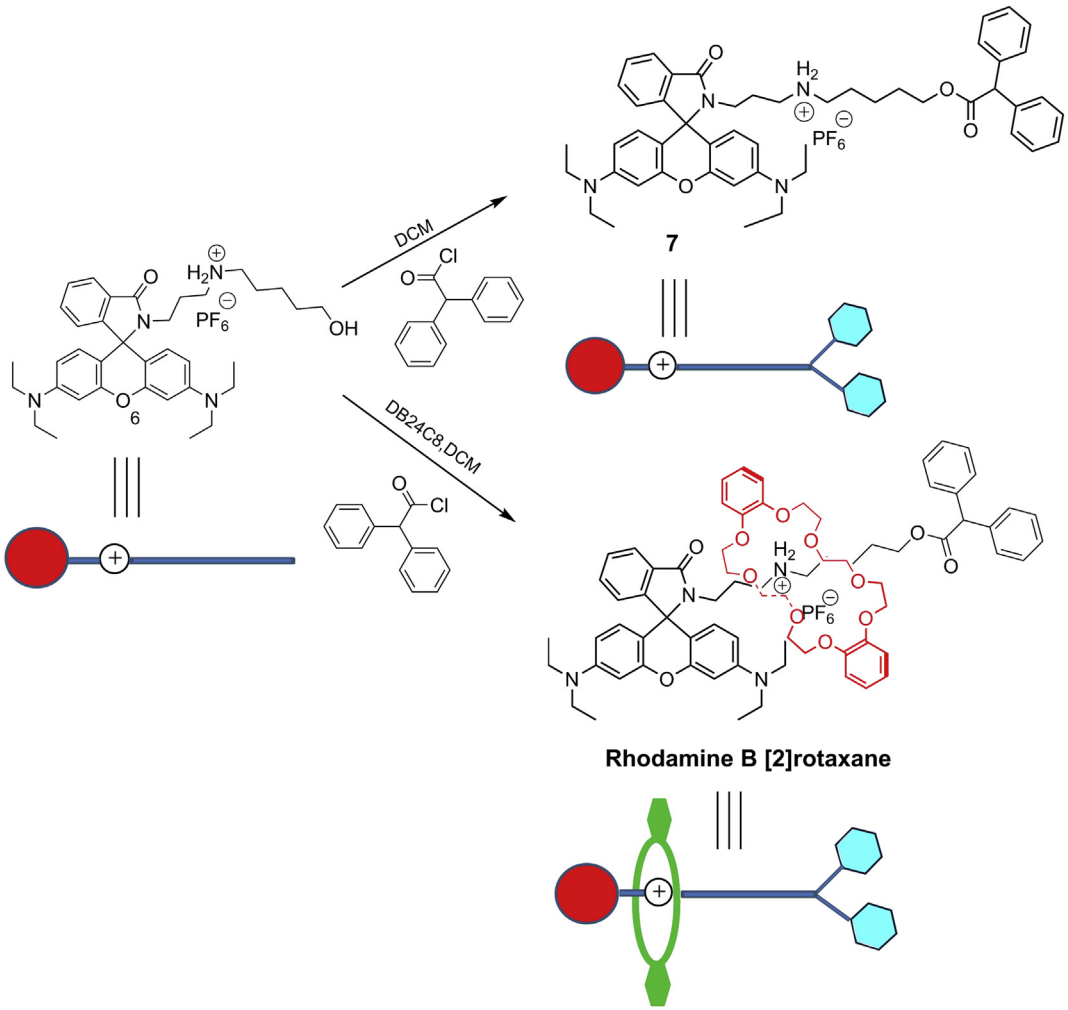

Scheme 3. The synthetic route for Rhodamine B [2]rotaxane.

For a better understanding of the conformation of the Rhodamine B [2]rotaxane, its energy optimized structure was obtained using Density functional theory (DFT) calculations with the B3LYP method using 6-31+G(d,p) as the basis set. The lowest energy structure of Rhodamine B [2]rotaxane was shown in Fig. 3, indicating that the DB24C8 ring was located around the *sec* -ammonium salt on the chain of the dumbbell of [2]rotaxane. These results combined with the HRMS spectrum (Fig. 4) confirmed the interlocking nature of Rhodamine B [2]rotaxane, which also indicates that this ionic template can synthesize good models for binary [2]rotaxane systems.

The UV–vis spectra of the macrocycle movement around the thread of compound **7** were compared by the addition of trifluoroacetic acid (TFA) and triethylamine (TEA). Absorption spectra of Rhodamine B [2]rotaxane were obtained upon titration with TFA in MeOH. As shown in Fig. 5, when no TFA was added to the solution containing [2]rotaxane, almost no absorbance above 546 nm could be observed, and the spectra exhibited two characteristic peaks belonging to Rhodamine B. However, a new strong absorbance band centered at 546 nm was observed upon addition of TFA, and this absorbance gradually increased with increasing TFA concentration, resulting in a color change from colorless to light pink. This indicates that Rhodamine B [2]rotaxane is a sensitive bistable model for TFA in MeOH. This phenomenon is primarily ascribed to the formation of the ring-opened amide form of Rhodamine B units on TFA (Scheme 4), based on our previous reports. In addition, the absorption peak at 546 nm rapidly increased with the addition of TFA to the solution, and the fluorescence intensity of Rhodamine B [2]rotaxane was enhanced to a moderate level after 6 equiv of TFA were added to the solution.

Having demonstrating the acid-based control over the position of DB24C8 on the axle of compound **7**, we also investigated using the position of the rotaxane macrocycle as a molecular switch in alkaline solution. The UV–vis spectra of the solutions containing Rhodamine B [2]rotaxane were observed with addition of TEA. The absorption changes for Rhodamine B [2]rotaxane in acidic and basic solutions are shown in Fig. 6. There was almost no difference between the curves of Rhodamine B [2] rotaxane and the solution with 10 equiv of TEA added. The curves of TFA were significantly different from those of Rhodamine B [2] rotaxane due to the ring-opened amide form of the Rhodamine B unit in rotaxane. After 20 equiv of TEA was added to the solution, this unit reverted back to its original state. The ring-opened amide form must have transitioned to a spirocyclic amide form after addition of TEA. However, the changes in the UV–vis spectra of Rhodamine B [2]rotaxane were very small in the acidic and basic solutions, and do not clearly confirm the position of the macrocyclic ring under different conditions. Further fluorescence spectra were obtained in MeOH to study the migration of the macrocyclic ring DB24C8.

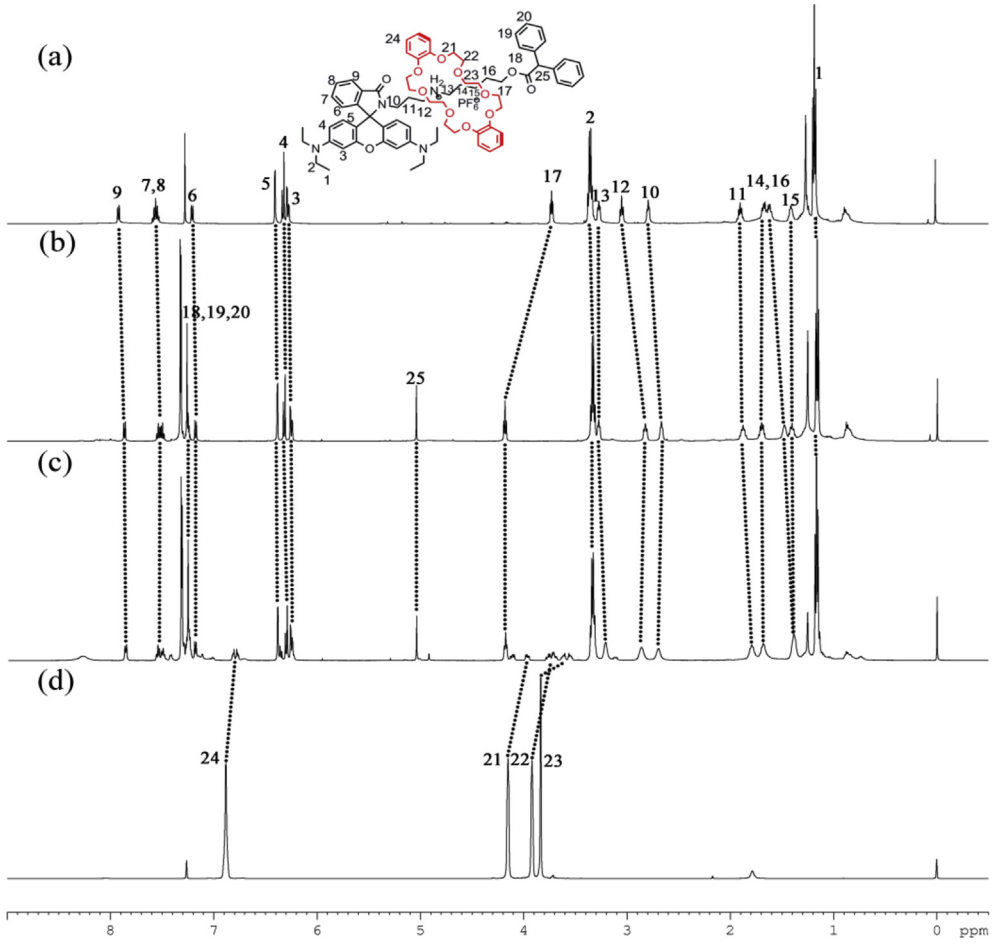

Fig. 2. Comparison of the ^{1}H NMR spectra (500 MHz, $CDCl_3$, 298K) of a), compound 6, b) compound 7, c) Rhodamine B [2]rotaxane, and d) DB24C8.

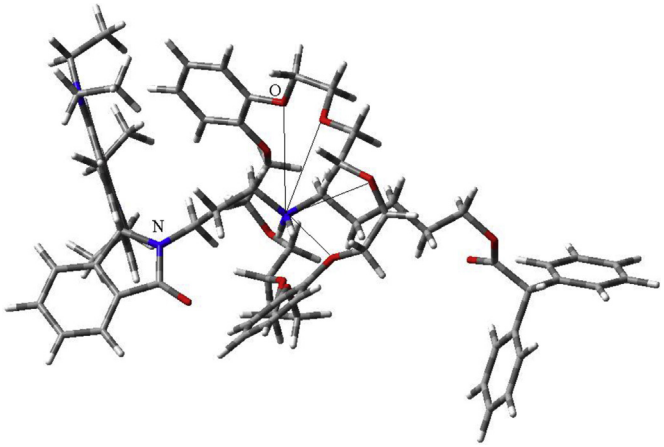

Fig. 3. Snapshot of a Gaussian simulation of Rhodamine B [2]rotaxane, illustrating the position of DB24C8 on the chain around the recognition site based on the intermolecular hydrogen bonding (line shown in Figure).

Changes in the fluorescence spectra of Rhodamine B [2]rotaxane under different pH conditions in methanol further investigated the movement of DB24C8 on the thread. These titration experiments were performed under the same conditions as the UV–vis experiments. As in the fluorescence spectroscopy experiments, Fig. 7 shows the appearance and increase in the emission peak of Rhodamine B at 576 nm, which was accompanied by a slight red shift upon addition of different volumes of TFA. These gradual changes were observed upon addition of up to 6 equiv of TFA, after, which the emission intensity remained unchanged. All of these data prove that the ring-opened amide form of the Rhodamine B moiety was formed in solution after the addition of TFA.

Fig. 8 displays the fluorescence spectra of Rhodamine B [2]rotaxane alone, with 10 equiv of added TEA, and with 10 and 20 equiv of added TFA and TEA. Rhodamine B [2]rotaxane exhibited stronger fluorescence (λ_{ex}=546 nm) at 576 nm than the other two curves. A similar but much more apparent band at 576 nm was observed upon titration with TEA. TEA can decrease the band at 576 nm. These changes in the fluorescence spectra can also be attributed to the movement of the DB24C8 macrocycle from the Rhodamine B unit towards the diphenylacetyl unit under irradiation. However, titration with 20 equiv of TEA to the solution containing Rhodamine B [2]rotaxane and 10 equiv of TFA resulted in a comparatively smaller decrease at 576 nm than in the free rotaxane solution. Overall, the DB24C8 ring could be shifted away from the Rhodamine B unit towards the other side by the addition of the solution under irradiation, and we monitored the location of the macrocycle through the changes in the fluorescence spectra. Hence, the relative position of the macrocycle on the thread was affected by the pH of the solution. At the same time, the theoretical basis for the synthesis of Rhodamine B [2]rotaxane confirms that the original state of DB24C8 resides near the recognition site of the

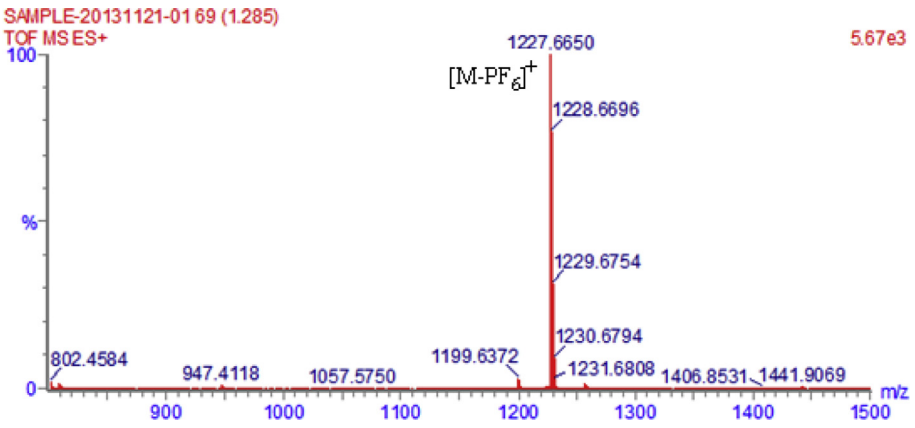

Fig. 4. HRMS of rhodamine B [2]rotaxane.

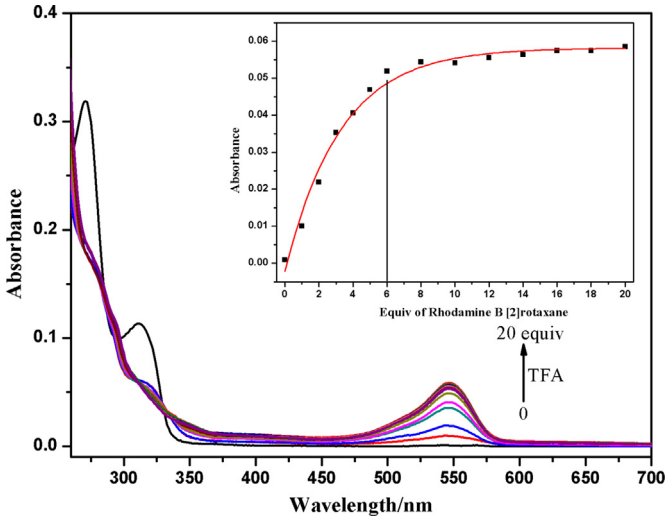

Fig. 5. UV–vis spectra of Rhodamine [2]rotaxane (10 μM) upon addition of different concentrations of trifluoroacetic acid (TFA). Inset: plot of the equivalent of TFA versus absorbance intensity at 546 nm.

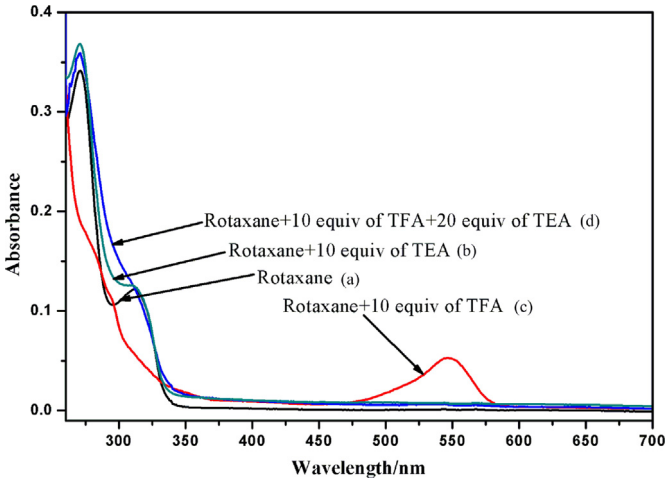

Fig. 6. UV–vis spectra of: (a) Rhodamine B [2]rotaxane (10 μM); (b) Rhodamine B [2] rotaxane (10 μM)+TEA (100 μM); (c) Rhodamine B [2]rotaxane (10 μM)+TFA (100 μM); (d) Rhodamine B [2]rotaxane (10 μM)+TEA (200 μM)+ TFA (100 μM).

thread. When TEA was added to the solution, the secondary ammonium salt lost an electron, which resulted in weaker hydrogen bonding between the recognition sites and the DB24C8 ring and led to the facile migration of the DB24C8 ring around Rhodamine B [2] rotaxane under irradiation. The pH-induced movement of Rhodamine B [2]rotaxane with TFA and TEA (input signals) under irradiation illustrates the application of this rotaxane as a molecular switch based on fluorescence intensity (output signals).

4. Conclusions

In summary, we constructed a novel Rhodamine B [2]rotaxane using a capping method that represents a new synthetic method to produce fluorescent rotaxanes. This capping method uses mild reaction conditions and simple steps and does not require a catalyst. This work will promote the construction of rotaxane systems and may lead to a wide range of applications. The effect of the variable pH value was also evaluated as a molecular switch, and this type of [2]rotaxane can serve as a model for molecular switches driven by light. The DB24C8 ring could be stimulated to shift from

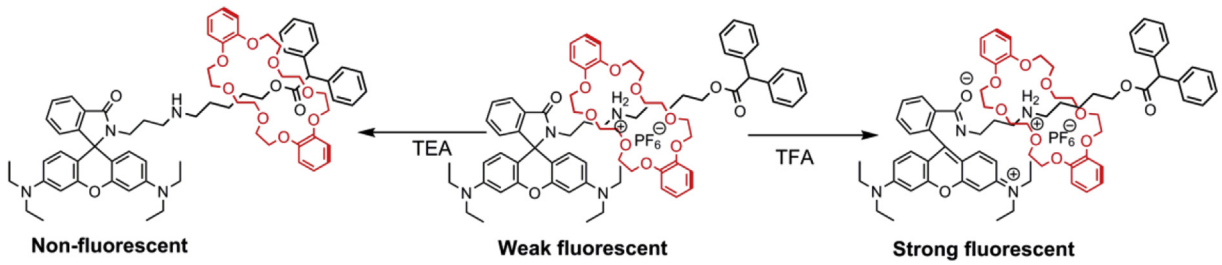

Scheme 4. Proposed machanism for addition of TFA and TEA to Rhodamine B[2]rotaxane.

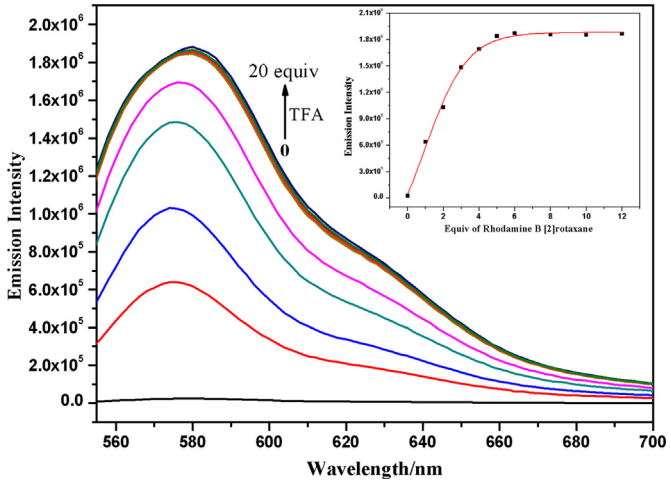

Fig. 7. Fluorescence spectra of Rhodamine B [2]rotaxane (10 μM) with different concentrations of TFA. Inset: plot of the fluorescence intensity versus the equivalent of TFA.

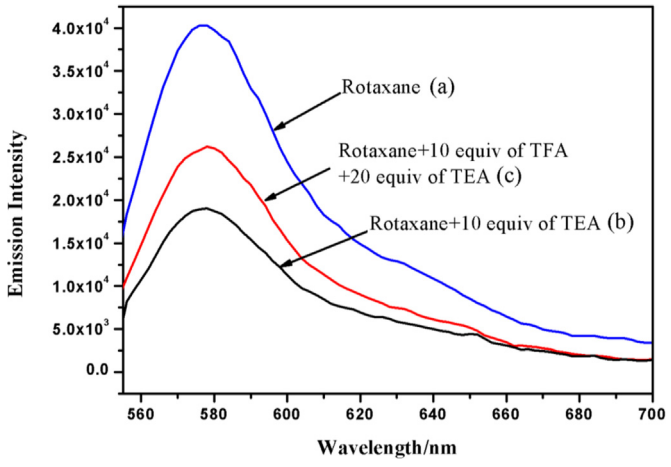

Fig. 8. Fluorescence spectra of: (a) Rhodamine B [2]rotaxane (10 μM); (b) Rhodamine B [2]rotaxane (10 μM)+TEA (100 μM); (c) Rhodamine B [2]rotaxane (10 μM)+TEA (200 μM)+ TFA (100 μM).

the Rhodamine B unit to the other stopper through irradiation, and the output signal was the fluorescence intensity, which can be easily detected compared to other spectral signals. This type of fluorescent [2]rotaxane has important potential applications in the construction of molecular switches with multi-output signals.

Acknowledgements

This research was supported by the National Natural Science Foundation of China (81371616), the Research Fund for the Doctoral Program of Higher Education of China (20133219120020) and the Jiangsu Specially Sponsored Professorship for Dr. Jing Zhu.

Supplementary data

Supplementary data related to this article can be found at http://dx.doi.org/10.1016/j.tet.2015.04.105.

References and notes

1. Lahlali, H.; Jobe, K.; Watkinson, M.; Goldup, S. M. *Angew. Chem., Int. Ed.* **2011**, *50*, 4151.
2. Dong, S. Y.; Han, C. Y.; Zheng, B.; Zhang, M. M.; Huang, F. H. *Tetrahedron Lett.* **2012**, *53*, 3668.
3. Brouwer, A. M.; Frochot, C.; Gatti, F. G.; Leigh, D. A.; Mottier, L.; Paolucci, F.; Rofþa, S.; Wurpel, G. W. *Science* **2001**, *291*, 2124.
4. Xue, M.; Yang, Y.; Chi, X. D.; Yan, X. Z.; Huang, F. H. *Chem. Rev.* **2015**, http://dx.doi.org/10.1021/cr5005869
5. Thomas, S. W.; Joly, G. D.; Swager, T. M. *Chem. Rev.* **2007**, *107*, 1339.
6. Li, S. J.; Liu, M.; Zhang, J. Q.; Zheng, B.; Wen, X. H.; Li, N.; Huang, F. H. *Eur. J. Org. Chem.* **2008**, *2008*, 6128.
7. Qu, D. H.; Ji, F. Y.; Wang, Q. C.; Tian, H. *Adv. Mater.* **2006**, *18*, 2035.
8. Leigh, D. A.; Morales, M.; Pérez, E. M.; Wong, J. K.; Saiz, C. G.; Slawin, A. M.; Carmichael, A. J.; Haddleton, D. M.; Brouwer, A. M.; Buma, W. J.; Wurpel, G. W. H.; Leon, S.; Zerbetto, F. *Angew. Chem., Int. Ed.* **2005**, *44*, 3062.
9. Qu, D. H.; Wang, Q. C.; Ren, J.; Tian, H. *Org. Lett.* **2004**, *6*, 2085.
10. Hsueh, S. Y.; Lai, C. C.; Chiu, S. H. *Chem.—Eur. J.* **2010**, *16*, 2997.
11. Whalley, A. C.; Seigerwald, M. L.; Guo, X.; Nuckolls, C. *J. Am. Chem. Soc.* **2007**, *129*, 12590.
12. Choi, J. W.; Flood, A. H.; Steuerman, D. W.; Nygaard, S.; Braunschweig, A. B.; Moonen, N. N.; Laursen, B. W.; Luo, Y.; Delonno, E.; Peters, A. J.; Jeppesen, J. O.; Xu, K.; Stoddart, J. F.; Heath, J. R. *Chem.—Eur. J.* **2006**, *12*, 261.
13. Zhu, J.; McFarland-Mancini, M.; Drew, A. F.; Smithrud, D. B. *Bioorg. Med. Chem. Lett.* **2009**, *19*, 520.
14. Zhu, J.; House, B. E.; Fleck, E.; Isaacsohn, I.; Drew, A. F.; Smithrud, D. B. *Bioorg. Med. Chem. Lett.* **2007**, *17*, 5058.
15. Zhu, J.; Smithrud, D. B. *Org. Biomol. Chem.* **2007**, *5*, 2992.
16. Berná, J.; Crowley, J. D.; Goldup, S. M.; Hänni, K. D.; Lee, A. L.; Leigh, D. A. *Angew. Chem., Int. Ed.* **2007**, *46*, 5709.
17. Lankshear, M. D.; Beer, P. D. *Coord. Chem. Rev.* **2006**, *250*, 3142.
18. Zhang, Z. B.; Han, C. Y.; Yu, G. C.; Huang, F. H. *Chem. Sci.* **2012**, *3*, 3026.
19. Cavallini, M.; Biscarini, F.; León, S.; Zerbetto, F.; Bottari, G.; Leigh, D. A. *Science* **2003**, *299*, 531.
20. Blanco, V.; Leigh, D. A.; Lewandowska, U.; Lewandowski, B.; Marcos, V. *J. Am. Chem. Soc.* **2014**, *136*, 4905.
21. Zhang, H.; Zhou, B.; Li, H.; Qu, D. H.; Tian, H. *J. Org. Chem.* **2012**, *78*, 2091.
22. Suzuki, S.; Ishiwari, F.; Nakazono, K.; Takata, T. *Chem. Commun.* **2012**, 6478.
23. Zhu, L. L.; Li, X.; Ji, F. Y.; Ma, X.; Wang, Q. C.; Tian, H. *Langmuir* **2009**, *25*, 3482.
24. Mateo-Alonso, A.; Ehli, C.; Guldi, D. M.; Prato, M. *Org. Lett.* **2012**, *15*, 84.
25. Zhang, H.; Hu, J.; Qu, D. H. *Org. Lett.* **2012**, *14*, 2334.
26. Ma, X.; Tian, H. *Chem. Soc. Rev.* **2010**, *39*, 70.
27. Pérez, E. M.; Dryden, D. T.; Leigh, D. A.; Teobaldi, G.; Zerbetto, F. *J. Am. Chem. Soc.* **2004**, *126*, 12210.
28. Cole, E. L.; Arunkumar, E.; Xiao, S.; Smith, B. A.; Smith, B. D. *Org. Biomol. Chem.* **2012**, *10*, 5769.
29. Li, Y.; Cao, L.; Tian, H. *J. Org. Chem.* **2006**, *71*, 8279.
30. Slater, B. J.; Davies, E. S.; Argent, S. P.; Nowell, H.; Lewis, W.; Blake, A. J.; Champness, N. R. *Chem.—Eur. J.* **2011**, *17*, 14746.
31. Yu, G.; Suzaki, Y.; Abe, T.; Osakada, K. *Dalton. T* **2013**, *42*, 1476.
32. Dong, S. Y.; Yuan, J. Y.; Huang, F. H. *Chem. Sci.* **2014**, *5*, 247.
33. Bao, X. F.; Liu, D. L.; Jin, Y. Y.; Liu, X. L.; Jiang, W. *RSC. Adv.* **2013**, *3*, 6783.
34. Zhang, C. J.; Li, S. J.; Zhang, J. Q.; Zhu, K. L.; Li, N.; Huang, F. H. *Org. Lett.* **2007**, *9*, 5553.
35. Li, Y.; Li, H.; Li, Y.; Liu, H.; Wang, S.; He, X.; Wang, N.; Zhu, D. *Org. Lett.* **2005**, *7*, 4835.
36. Oddy, F. E.; Brovelli, S.; Stone, M. T.; Klotz, E. J.; Cacialli, F.; Anderson, H. L. *J. Mater. Chem.* **2009**, *19*, 2846.
37. Yamauchi, K.; Miyawaki, A.; Takashima, Y.; Yamaguchi, H.; Harada, A. *J. Org. Chem.* **2010**, *75*, 1040.
38. Lagona, J.; Mukhopadhyay, P.; Chakrabarti, S.; Isaacs, L. *Angew. Chem., Int. Ed.* **2005**, *44*, 4844.
39. Fang, L.; Olson, M. A.; Benítez, D.; Tkatchouk, E.; Goddard, W. A., III; Stoddart, J. F. *Chem. Soc. Rev.* **2010**, *39*, 17.
40. Zhao, Y. L.; Aprahamian, I.; Trabolsi, A.; Erina, N.; Stoddart, J. F. *J. Am. Chem. Soc.* **2008**, *130*, 6348.
41. Wang, F.; Zhou, Q. Z.; Zhu, K. L.; Li, S. J.; Wang, C.; Liu, M.; Li, N.; Fronceek, F. R.; Huang, F. H. *Tetrahedron* **2009**, *65*, 1488.
42. Wei, P. F.; Yan, X. Z.; Li, J. Y.; Ma, Y. J.; Yao, Y.; Huang, F. H. *Tetrahedron* **2012**, *68*, 9179.
43. Bao, X. F.; Isaacsohn, I.; Drew, A. F.; Smithrud, D. B. *J. Am. Chem. Soc.* **2006**, *128*, 12229.
44. Bao, X. F.; Isaacsohn, I.; Drew, A. F.; Smithrud, D. B. *J. Org. Chem.* **2007**, *72*, 3988.